The electrochemical reduction kinetics of oxygen in dimethylsulfoxide

Hendi, Ruba; Robbs, Peter H.; Sampson, Beatrice; Pearce, Ryan; Rees, Neil V.

DOI:
10.1016/j.jelechem.2018.09.052

Document Version
Publisher's PDF, also known as Version of record

Citation for published version (Harvard):
Hendi, R, Robbs, PH, Sampson, B, Pearce, R & Rees, NV 2018, 'The electrochemical reduction kinetics of oxygen in dimethylsulfoxide', *Journal of Electroanalytical Chemistry*, vol. 829, pp. 16-19. https://doi.org/10.1016/j.jelechem.2018.09.052

Journal of Electroanalytical Chemistry 829 (2018) 16–19

Contents lists available at ScienceDirect

Journal of Electroanalytical Chemistry

journal homepage: www.elsevier.com/locate/jelechem

The electrochemical reduction kinetics of oxygen in dimethylsulfoxide

Ruba Hendi, Peter H. Robbs, Beatrice Sampson, Ryan Pearce, Neil V. Rees*

School of Chemical Engineering, University of Birmingham, Edgbaston, Birmingham B15 2TT, United Kingdom

ARTICLE INFO

Keywords:
Reduction
Oxygen
DMSO
Kinetics
Marcus-Hush
Butler-Volmer
Outer-sphere

ABSTRACT

The quasi-reversible one-electron reduction of oxygen in dimethylsulfoxide is reported for a range of electrode materials (C, Pt, Pd, and Au) and temperatures (293–343 K). Modelling was undertaken using Butler-Volmer and symmetric Marcus-Hush methods, with the former found to provide more reproducible results for this system, in agreement with previous reports of quasi-reversible systems. The reorganisation energy for the reaction was found to be ca. 1.0 eV, and the reaction confirmed to be predominantly outer-sphere. The observed standard electrochemical rate constant (k_0) is ca. 5.7 times faster for C electrodes than Pt, despite having a lower electronic density of states.

1. Introduction

The oxygen reduction reaction (ORR) is of fundamental importance to many electrochemical energy applications, for example metal-air batteries and fuel cells. In the case of reactive metal-air (or oxygen) batteries, aprotic solvents are commonplace and dimethyl sulfoxide (DMSO) is widely used [1,2]. A detailed understanding of the kinetics of oxygen reduction in DMSO is therefore desirable, including any effects of electrode material on the kinetics. It is anticipated that such studies may help inform aspects of (metal-air) battery and fuel cell design.

Furthermore, the complexity of the aqueous ORR has led some workers to seek proxy systems, especially for theoretical studies where aprotic solvents provide the simplest ORR, with quasi-reversible one electron transfer (Eq. (1)). DMSO is an interesting experimental system due to its miscibility with water and potential for mixed-solvent ORR studies.

$$O_2 + e^- \rightleftarrows O_2^- \tag{1}$$

For the one-step electron reduction of oxygen the kinetics can be most easily described using either the Butler-Volmer or Marcus-Hush approaches [3]. The ubiquitous Butler-Volmer model relates the reductive and oxidative electron transfer rate constants for Eq. (1), to the overpotential ($E - E_f^0$) via a transfer coefficient (α or β) and a standard heterogeneous electrochemical rate constant (k_0):

$$k_{red} = k_0 exp\left[\frac{-\alpha F(E - E_f^0)}{RT}\right] \tag{2}$$

and

$$k_{ox} = k_0 exp\left[\frac{+\beta F(E - E_f^0)}{RT}\right] \tag{3}$$

where F is Faraday's constant, R the universal gas constant and T the absolute temperature.

The symmetric Marcus-Hush (SMH) model has become increasingly used to gain insight into the physical process at the molecular level [4–8]; in the case of a diffusional outer-sphere electron transfer process, the SMH defines the standard electrochemical rate constant, k_0, as:

$$k_0 = \frac{2\pi^{3/2}\rho\ |H_{DA}|^2}{\beta h \Lambda^{1/2}} exp\left(-\frac{\Lambda}{4}\right) I(0, \Lambda) \tag{4}$$

where ρ is the density of electronic states of the electrode material, H_{DA} is the electronic coupling matrix between the electrode and electroactive species (donor and acceptor) at their closest distance of approach, β in this context is the electronic coupling attenuation coefficient (linked to H_{DA}), and h is Planck's constant [7,8]. The parameters Λ and $I(0, \Lambda)$ are given by:

$$\Lambda = \frac{F}{RT}\lambda \tag{5}$$

and

$$I(\theta, \Lambda) = \int_{-\infty}^{\infty} \frac{exp\left\{-\frac{(\varepsilon - \theta)^2}{4\Lambda}\right\}}{2\,cosh\left(\frac{\varepsilon}{2}\right)} d\varepsilon \tag{6}$$

where

* Corresponding author.
E-mail address: n.rees@bham.ac.uk (N.V. Rees).

https://doi.org/10.1016/j.jelechem.2018.09.052
Received 25 July 2018; Received in revised form 26 September 2018; Accepted 27 September 2018
Available online 02 October 2018

$$\theta = \frac{F}{RT}(E - E_f^0) \tag{7}$$

and where λ is the Marcus reorganisation energy and ε is an electronic state, with k_0 defined at $\theta = 0$. [7,8]

The one-electron reduction of dioxygen to superoxide is usually treated as an outer-sphere electron transfer, regardless of electrode material or solvent [9]. Here we report a study of the electro-reduction kinetics of oxygen dissolved in DMSO, varying electrode material and temperature to determine the reorganisation energy of Eq. (1) and the source of material-effects on the kinetics in the absence of a classical surface-analyte bond (inner sphere) interaction.

2. Experimental

The following chemicals and gases were obtained commercially and used without further purification: potassium chloride (Sigma Aldrich, > 99%), hexaammineruthenium (III) chloride (Sigma Aldrich, > 99%), tetra-*n*-butylammonium perchlorate, (TBAP, Fluka, < 99%), potassium nitrate (Sigma Aldrich > 99.99%), dimethyl sulfoxide (DMSO, Sigma Aldrich > 99%), nitrogen (oxygen-free, BOC Gases plc), and oxygen (N5 grade, BOC Gases plc). DMSO was stored over molecular sieves prior to use.

All solutions were made with sufficient inert electrolyte to be fully supported and thoroughly purged with either nitrogen or oxygen as appropriate. In addition, the aqueous solutions used for electrochemical calibration of electrodes were made with ultrapure water of resistivity not < 18.2 MΩ·cm (milliQ, Millipore). Variable temperature experiments were conducted by heating the solution in a thermostatted water bath (with the reference electrode within the thermostatted reaction cell), with temperature measurements confirmed via a mercury thermometer.

Electrochemical measurements were made using a three electrode arrangement in a faraday cage, controlled by a PGStat128N potentiostat (Metrohm-Autolab BV, Utrecht, NL). A saturated Ag/AgCl leakless reference electrode and bright platinum mesh counter electrode were used. The working microelectrodes used were carbon, platinum (both from BASI Inc.), platinum and palladium (both fabricated in-house), and were all of microwire-in-glass construction. The radii of the working microelectrodes employed were confirmed via steady state linear sweep voltammetry of the reduction of 1 mM hexaammineruthenium(III) chloride in 0.1 M KNO_3, and were calculated to be as follows: C 4.8 μm, Pt 5.0 μm, Pd 12.2 μm, and Au 10.9 μm. A Pt macroelectrode (radius 2.5 mm) was used for diffusion coefficient measurements.

3. Results & discussion

First, linear sweep voltammetry (LSV) was used to determine the diffusion coefficients and saturated concentration of dioxygen in DMSO at different temperatures using a Pt microelectrode and macroelectrode. The measured steady-state limiting and peak currents (I_{Lim} and I_P respectively) from these scans were compared to determine the diffusion coefficient, D, according to Eqs. (1)–(3) for a $1e^-$ transfer [3].

$$I_{Lim} = 4FCDr_d \tag{8}$$

$$I_p = (2.99 \times 10^5)\pi R^2 C(\alpha D\nu)^{1/2} \tag{9}$$

Therefore

$$\frac{I_{Lim}}{I_p} = 0.411\left(\frac{r_d}{R^2}\right)\left(\frac{D}{\alpha\nu}\right)^{1/2} \tag{10}$$

where F is the Faraday constant, r_d is the microdisk radius, R is the macrodisk radius, α is the transfer coefficient and ν is the voltage scan rate (here 25 mV s^{-1}). The value of α was determined from a Tafel plot of the Pt macroelectrode LSV and confirmed through modelling of the Pt microelectrode LSV to be 0.36. The values of D and $[O_2]_{sat}$ over the temperature range 293–343 K are shown in Fig. 1 below.

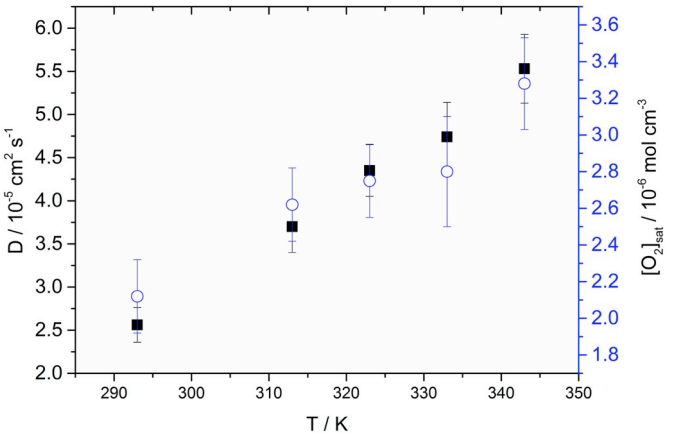

Fig. 1. The variation of diffusion coefficient of oxygen (■) and $[O_2]_{sat}$ (○) with temperature in a solution of 0.1 M TBAP in DMSO.

These results are consistent with literature values for $[O_2]_{sat}$ at 298 K of 2.1 mM [10]. Literature reports for diffusion coefficients across that temperature range from 2.2×10^{-5} to 7.49×10^{-5} $cm^2 s^{-1}$ [10–13]. An Arrhenius-type plot of the data in Fig. 1 yields a gradient of 1.53×10^3 K^{-1} ($R^2 = 0.991$), corresponding to an activation energy for diffusion of ca. 12.7 kJ mol^{-1}.

Next, the LSV for the reduction of oxygen in DMSO was recorded at: (i) carbon, platinum, gold, and palladium microelectrodes at 293 K, and (ii) carbon and platinum microelectrodes at a range of temperatures between 293 K and 343 K.

The voltammetry was then modelled via commercial software (DigiElch™) which is capable of modelling experimental data via either Butler-Volmer, or symmetric Marcus-Hush algorithms. Simulations were performed using both methods for comparison in order to determine the optimal model to use [7,8], and these are detailed in the Supporting Information along with a selection of 'best-fits' to experimental data.

In brief it was found that the SMH model gave inconsistent results, which we ascribe to the known difficulties in fitting quasi-reversible and irreversible voltammetry to the symmetric MH model [8,14–17]. We therefore proceeded with the Butler-Volmer simulation to extract values for the standard electrochemical rate constant (k_0), transfer coefficient (α), and formal potential (E_f^0). Table 1 shows the fitted parameters – the variation in formal potential is ascribed to 'drift' on the aqueous reference electrode.

Fig. 2(a) illustrates the variation in k_0 with electrode material at

Table 1
Fitted BV parameters for variable temperature linear sweep voltammetry of oxygen reduction at 4 different electrode materials.

T/K	Platinum			Carbon		
	$k_0/10^{-3}$ cm s^{-1}	α	E_f^0/V	$k_0/10^{-2}$ cm s^{-1}	α	E_f^0/V
293	7.5	0.36	−0.520	4.3	0.41	−0.495
303	10.0	0.34	−0.460	6.2	0.42	−0.366
313	14.0	0.37	−0.340	8.0	0.42	−0.270
323	20.0	0.33	−0.365	9.9	0.39	−0.270
333	–	–	–	13.5	0.39	−0.315
343	30.0	0.44	−0.360	17.5	0.36	−0.330

	Palladium			Gold		
	$k_0/10^{-3}$ cm s^{-1}	α	E_f^0/V	$k_0/10^{-3}$ cm s^{-1}	α	E_f^0/V
293	4.0	0.35	−0.755	6.0	0.39	−0.500

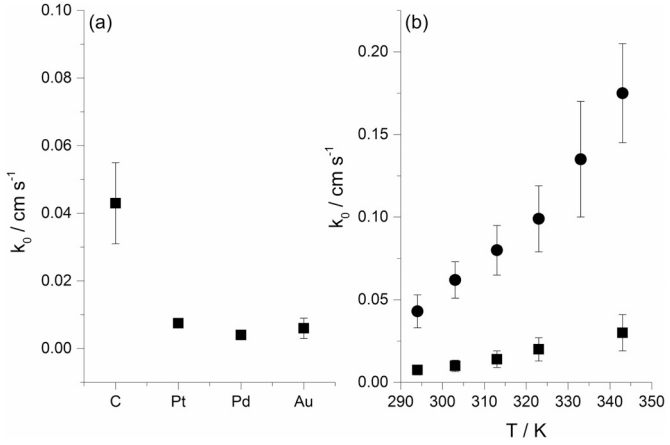

Fig. 2. (a) The variation of k_0 with electrode material at 293 K, and (b) a comparison of k_0 values for Pt (■) and C (●) across the temperature range.

293 K, the values for transfer coefficient being approximately within experimental error of each other. The literature only reports values for the reduction of oxygen on glassy carbon and graphite [10,11], and finds k_0 values of 3.2 to 9.3 × 10^{-2} cm s^{-1} and 2.75 × 10^{-2} cm s^{-1} respectively, which are in good agreement with the value found here for a carbon fibre microelectrode. It is noticeable from Fig. 2 that the rate constants for oxygen reduction at the metallic electrodes are approximately within experimental error of each other, whilst the rate constant for carbon is significantly higher. This latter observation is similar to that by Nissim et al. [18] where the heterogeneous rate constant for the reduction of a series of quinones in acetonitrile also showed a clear dependence on the electrode material.

To confirm that the reduction is outer-sphere at both surfaces, plot of the variable temperature data was constructed and shown in Fig. 3. Combining Eqs. (4) and (5):

$$\ln k_0 = -\frac{\lambda F}{4RT} + ln\left\{\frac{2\pi^{3/2}\rho\ |H_{DA}|^2}{\beta h \Lambda^{1/2}} I(0,\Lambda)\right\} \tag{11}$$

yields approximately equal gradients for Pt and C of −2.92 × 10^3 K^{-1} and −2.79 × 10^3 K^{-1} respectively which, using Eq. (11), correspond to reorganisation energies (λ) of 1.00 eV (97.1 kJ mol^{-1}) and 0.96 eV (92.8 kJ mol^{-1}).

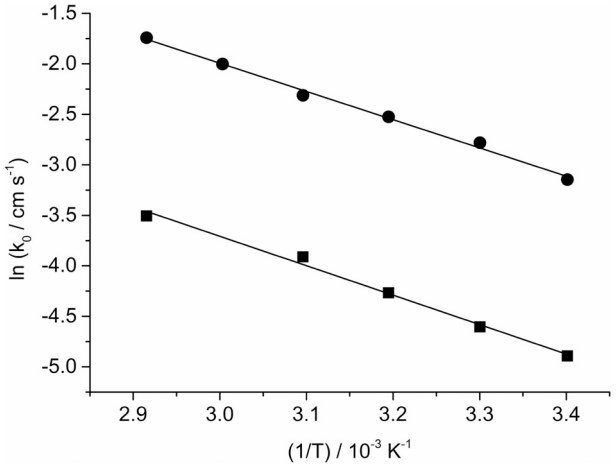

Fig. 3. The temperature variation of k_0 on Pt (■) and C (●) microelectrode surfaces plotted according to Eqs. (4) & (5). The gradients of these plots are −2.92 × 10^3 K^{-1} (R^2 = 0.991) and −2.79 × 10^3 K^{-1} (R^2 = 0.994) respectively. Error bars present in Fig. 2 have been omitted here for simplicity.

This observation strongly suggests that the reorganisation energy is dominated by solvent reorganisation and hence the reduction is outer-sphere in nature. For comparison, Hartnig and Koper [9], modelled the first reduction step of dioxygen in aqueous media via DFT and concluded that it is outer-sphere with values for the inner and outer-sphere components of the reorganisation energy of 10 kJ mol^{-1} and 60–80 kJ mol^{-1} respectively.

In many cases, the solvent reorganisation energy (λ_{os}) is calculated via the Born solvation energy [19]:

$$\lambda_{os} = \frac{e^2\gamma}{8\pi\varepsilon_0}\left(\frac{1}{a} - \frac{1}{2d}\right) \tag{12}$$

where e is the electronic charge, ε_0 is the permittivity of free space, γ is the solvent Pekar factor (=0.437 for DMSO [20]), a is the molecular radius and d the distance from the plane of reaction to the electrode surface (commonly taken as ∞ following Hale [21]).

The molecular radius in Eq. (11) is often taken as the solvodynamic radius [22–25] derived from the measured diffusion coefficient and the Stokes-Einstein equation:

$$D = \frac{k_B T}{P\pi\eta a} \tag{13}$$

where k_B is the Boltzmann constant, T the absolute temperature, and η the solvent viscosity (1.996 mPa·s for DMSO [20]). Here P is a constant that depends on the shape and relative size of the solute molecule: the most commonly-used limiting values of 4 and 6 relate to a spherical molecule that is either of a similar size to the solvent molecules, or considerably larger [26]. In the present case, however, the oxygen molecule is smaller than solvating molecules: Eyring proposed using P values as low as 1 for such cases of small-molecule diffusion [27], but this is not widely adopted and studies generally report empirical relationships for specific solute-solvent combinations that account for the observed diffusion coefficient values [26,28–30].

The observed mean solvent reorganisation energy of 0.98 eV (Fig. 3) implies a = 3.21 Å (at 293 K) via Eq. (12) and therefore P = 1.276. This molecular radius compares with the Van der Waals radius of 1.52 Å [31], and the radius derived from molecular volumes of 3.03 Å [28,30]. This highlights the limitations of the application of Eqs. (12) and (13) to cases of small molecule diffusion – the breakdown of the solvent-continuum model manifests itself as inaccurate λ_{os} and a values, and indicates that stochastic models are required.

Since the electron transfer is overwhelmingly outer-sphere in nature, differences in the observed standard heterogeneous rate constant are due to the pre-exponential factor in Eq. (4), and hence the ratio of the values of k_0 for C and Pt (ca. 5.7 ± 0.7) is governed by:

$$\frac{k_0(C)}{k_0(Pt)} = \frac{\rho(C)|H_{DA}(C)|^2\beta(Pt)}{\rho(Pt)|H_{DA}(Pt)|^2\beta(C)} \tag{14}$$

In order to quantify the relative density of states (DoS, ρ) in this study, it was necessary to measure the potential of zero charge of both electrodes in the electrolyte solution (see Supporting Information). Therefore, cyclic voltammograms were recorded at a scan rate of 25 mV s^{-1} at a range of potentials in a solution of 0.1 M TBAP in DMSO which had been thoroughly purged with nitrogen. By measuring the capacitative current and finding its minimum value [18], the potentials of zero charge were estimated to be +0.55 V and +0.80 V for Pt and C electrodes respectively, leading to values of ($E_f^0 - E_{pzc}$) at 293 K of −1.07 V (Pt) and −1.295 V (C). The corresponding densities of states at these potentials for graphitic C is in the range of 0.08 states $atom^{-1}$ eV^{-1} [32], whereas the DoS for Pt is ca. 1.15 states $atom^{-1}$ eV^{-1} [33,34], comprising of *sp*-, and *d*-band contributions of approximately 0.3, and 0.85 states $atom^{-1}$ eV^{-1} respectively [33].

The relevance of which orbital bands contribute to the DoS was highlighted by Gosavi and Marcus [34], who showed that the rate of non-adiabatic electron transfer is not linearly proportional to the total

DoS; rather for a detailed understanding of the source of the difference in k_0, it is necessary to consider the individual electronic coupling elements (H_{DA}) for each of the bands. They reported the relative effectiveness of the *sp*-band states was 11.2 times greater than the *d*-states, despite the *d* electrons being at the Fermi level [34]: the *d*-band generally couples weakly to the outside environment and so it has little influence over the electrochemical rate constant [34].

Hence we conclude that the k_0(C) / k_0(Pt) ratio is determined by the *sp*-bands, the matrix elements for their (donor-acceptor) coupling with a reactant oxygen molecule, and associated attenuation coefficients (β). The reported specific adsorption of DMSO onto Pt and Au electrodes will undoubtedly have an effect [35] upon the plane of closest approach of reactants. The effect on solvent on the kinetics is clearly significant even where the reactant is common and the electrode material varies: for example in the aqueous electrochemistry of oxygen k_0(Pt) > k_0(C). The dielectric properties of the solvent as well as the structure of the electrode-solution interface (including specific vs. non-specific adsorption) can have profound effects on the energetics of electron transfer.

4. Conclusions

The reduction of oxygen in DMSO has been shown to proceed via a predominantly outer-sphere mechanism with an activation energy of 0.98 ± 0.02 eV, and has some sensitivity to the electrode surface material. The heterogeneous rate constant is nearly 6 times faster on graphitic carbon fibre than Pt, Pd or Au, despite the metallic electrodes having a higher total electronic density of states at the formal potential. The rate appears to be determined by a combination of (i) the relative densities of states of the *sp*-bands (not the total DoS), and the coupling matrix elements of them to the oxygen (acceptor), and (ii) the attenuation coefficients and possible effects of specific adsorption.

Acknowledgements

The authors thank EPSRC (EP/G037116/1) for funding.

Appendix A. Supplementary data

Supplementary data to this article can be found online at https://doi.org/10.1016/j.jelechem.2018.09.052.

References

[1] Q. Yu, S. Ye, J. Phys. Chem. C 119 (2015) 12236.
[2] P. Reinsberg, A. Weiß, P.P. Bawol, H. Baltruschat, J. Phys. Chem. C 121 (2017) 7677.
[3] A.J. Bard, L.R. Faulkner, Electrochemical Methods: Fundamentals and Applications, 2nd Ed., Wiley, New York, 2001.
[4] R.A. Marcus, J. Chem. Phys. 43 (1965) 679.
[5] S. Fletcher, J. Solid State Electrochem. 14 (2010) 705.
[6] C.E.D. Chidsey, Science 251 (1991) 919.
[7] S.W. Feldberg, Anal. Chem. 82 (2010) 5176.
[8] M.C. Henstridge, E. Laborda, N.V. Rees, R.G. Compton, Electrochim. Acta 84 (2012) 12.
[9] C. Hartnig, M. Koper, J. Electroanal. Chem. 532 (2002) 165.
[10] D. Vasudevan, H. Wendt, J. Electroanal. Chem. 192 (1995) 69.
[11] M.E. Ortiz, L.J. Nunez-Vergara, J.A. Squella, J. Electroanal. Chem. 549 (2003) 157.
[12] D.T. Sawyer, G. Chiercato Jr., C.T. Angelis, E.J. Nanni Jr., T. Tsuchiya, Anal. Chem. 54 (1982) 1720.
[13] J.D. Wadhawan, P.J. Welford, H.B. McPeak, C.E.W. Hahn, R.G. Compton, Sensors Actuators B 88 (2003) 40.
[14] D. Suwatchara, N.V. Rees, M.C. Henstridge, E. Laborda, R.G. Compton, J. Electroanal. Chem. 665 (2012) 38.
[15] D. Suwatchara, M.C. Henstridge, N.V. Rees, R.G. Compton, J. Phys. Chem. C 115 (2011) 14876–14882.
[16] E. Laborda, C. Batchelor-McAuley, D. Suwatchara, M.C. Henstridge, R.G. Compton, J. Electroanal. Chem. 694 (2013) 30.
[17] E. Laborda, Y. Wang, M.C. Henstridge, F. Martinez-Ortiz, A. Molina, R.G. Compton, Chem. Phys. Lett. 512 (2011) 133–157.
[18] R. Nissim, C. Batchelor-McAuley, R.G. Compton, Chem. Commun. 48 (2012) 3294.
[19] J.O'.M. Bockris, S.U.M. Khan, Surface Electrochemistry, Plenum Press, New York, 1993.
[20] W.R. Fawcett, C.A. Foss Jr., Electrochim. Acta 36 (1991) 1767.
[21] J.M. Hale, N.S. Hush (Ed.), Reactions of Molecules at Electrodes, Wiley, London, 1971.
[22] A.D. Clegg, N.V. Rees, O.V. Klymenko, R.G. Compton, J. Am. Chem. Soc. 126 (2004) 6185.
[23] A.D. Clegg, N.V. Rees, O.V. Klymenko, R.G. Compton, ChemPhysChem 5 (2004) 1234.
[24] N.V. Rees, A.D. Clegg, O.V. Klymenko, R.G. Compton, J. Phys. Chem. B 108 (2004) 13047.
[25] A.D. Clegg, N.V. Rees, O.V. Klymenko, R.G. Compton, J. Electroanal. Chem. 580 (2005) 78.
[26] J.T. Edward, J. Chem. Educ. 47 (1970) 261.
[27] S. Glasstone, H. Eyring, K.J. Laidler, The Theory of Rate Processes, McGraw-Hill, 1941.
[28] D.M. Himmelblau Chem, Rev. 64 (1964) 527.
[29] R.K. Murarka, S. Bhattacharyya, B. Bagchi, J. Chem. Phys. 117 (2002) 10730.
[30] J.C.M. Li, P. Chang, J. Chem. Phys. 23 (1955) 518.
[31] CRC Handbook of Chemistry & Physics, 95th ed., CRC Press, 2014.
[32] J.R. Dahn, J.N. Reimers, A.K. Sleigh, T. Tiedje, Phys. Rev. B 45 (1992) 3773.
[33] D.A. Papconstantopoulos, Handbook of the Band Structure of Elemental Solids, Plenum Press, New York, 1986.
[34] S. Gosavi, R.A. Marcus, J. Phys. Chem. B 104 (2000) 2067.
[35] J. Sobkowski, M. Szklarczyk, Electrochim. Acta 25 (1980) 383.